Journal of Rehabilitation in Civil Engineering 7-4 (2019) 18-36

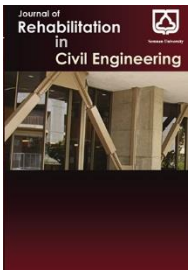

Journal homepage: http://civiljournal.semnan.ac.ir/

Estimation of the Elastic Properties of Important Calcium Silicate Hydrates in Nano Scale - a Molecular Dynamics Approach

A. Tarighat[1] and D. Tavakoli[2*]
1. Department of Civil Engineering, Shahid Rajaee Teacher Training University, Tehran, Iran
2. Department of Civil Engineering, Shahrekord University, Shahrekord, Iran

Corresponding author: *d.tavakoli@sru.ac.ir*

ARTICLE INFO

Article history:
Received: 14 May 2018
Accepted: 14 July 2018

Keywords:
Calcium Silicate Hydrates,
Mechanical Properties,
Molecular Dynamics Simulation,
Nano-Scale.

ABSTRACT

Approximately, 50 to 70 percent of hydration products in hydrated cement paste are polymorphisms of C-S-H gel. It is highly influential in the final properties of hardened cement paste. Distinguishing C-S-H nano-structure significantly leads to determine its macro scale ensemble properties. In this paper, a nono-scale modeling is employed. In order to carry it out, the major C-S-H compounds, with a vast range ratios of Ca/Si from 0.5 to 3 were selected and applied in different simulations. These materials included tobermorite 9Å, tobermorite 11Å, tobermorite 14Å, clinotobermorite, jennite, afwillite, okenite, jaffeite, foshagite, and wollastonite. Furthermore, the molecular dynamics method was employed to evaluate some consequential mechanical properties such as bulk modulus, shear modulus, Young's modulus and poisson ratio. Five different force fields (COMPASS, COMPASS II, ClayFF, INTERFACE and Universal) were applied and compared with each other to be able to measure the mechanical properties of these compounds. Lastly, the properties of two types of C-S-H with high and low density were computed using Mori-Tanaka method. The main aim of this paper is to distinguish the most similar natural C-S-H material to C-S-H from cement hydration and finding appropriate force filed.

1. Introduction

Approximately, the whole usage of concrete in one year would be more than one ton per person in the world. Thus, doing research about applying modern technologies to inquire nano-structure of concrete is crucial [1,2].

Given the importance of concrete and cement-based materials, numerous studies,

DOI: 10.22075/JRCE.2018.14821.1273

both experimental and theoretical, have been conducted. Cement paste plays a significant role in the concrete properties. Any defect in cement paste might lead to considerable alternation to concrete properties. Considering this matter,a great extent of concrete research is focused on the cement paste. The mixture of water and cement forms cement paste and it has own properties. These properties stem from formation of hydration products in the cement hardened paste. Cement hydration products mostly include: Calcium-Silicate-Hydrate (C-S-H) gel, Calcium Hydroxide (CH), AFt and AFm phases (Ettringite, Monosulfate, Monocarbonate and etc.) and residual unhydrated cement. These compounds, with their different nano structures and properties, lead to a complicated and inhomogeneous nano structure of hydrated cement paste. The major component of hydrated cement paste that has a significant role in its mechanical properties is C-H-S gel. Given the structure of C-S-H gel and the extensive amount of it in cement paste, a remarkable amount of cement hardened paste properties depends on it [3]. Therefore, inspecting C-S-H gel is essential in knowing the cement paste properties and, at a larger scale, concrete properties. Despite this importance, the structure of C-S-H gel is not adequately known and theoretical and experimental research studies still go on.

In order to know more about the C-S-H gel and ameliorate concrete nano- or -micro structure and also to remove any defects, the nano-structure C-S-H required to be explored adequately. Knowing its nano-structure and removing its defects, any damage in its macro structure would be prevented and the concrete quality and lifetime would also increase [4-6]. As a result of the lack of recognition of exact structure of C-S-H and lack of natural access to it, some of natural materials that have similar structures are examined to be able to study the C-S-H [7]. The most popular materials that have a similar structure to cement paste C-S-H are tobermorite family and jennite. Other similar materials are jaffeite, okenite, afwillite, foshagite, and wollastonite [8].

Contemplating experimental methods limitations and also the importance of finding out the nano-scale of materials, employing simulation methods at nano-scale might be beneficial to know about the nano structure and properties of materials similar to C-S-H. The literature results have indicated that the molecular dynamics is a very effective method to simulate different compounds and it also has had a suitable performance in terms of mechanical properties [9]. This method has recently been applied for different structures and scientific works [10-14]. In the present study, the same method was employed in order to inquire the C-S-H nano structure.

There are few studies focusing the estimation of C-S-H mechanical properties using experimental methods. In some of them, nanoindentation experiments were applied to compute the Young's modulus and also concrete Poisson's ratio [15-18]. Similarly, in a study, XRD method was used to determine the properties of tobermorite [19].

The cement paste numerical simulation in nano scale is a newly-fledged field and the investigation of cement paste nano structure has recently been demonstrated. Applying MD to simulate the nano structure of C-S-H was inspected by Faucon et. al [20]. They studied C-S-H nano structures at Ca/Si ratios between 0.66 and 0.83. Manzano et al., could

determine the mechanical properties of cement paste by energy minimization via molecular mechanics [8]. Subramani et al. also inquired the mechanical properties of C-S-H gel via molecular dynamics. They modeled tobermorite and foshagite and examined the attack of magnesium ions to cement paste. They also computed the potential energy of C-S-H equivalent crystal structure through applying molecular statics [21]. Murray et al, also investigated the stress-strain relationship of C-S-H gel with the offered structure of Subramani [22]. Various atomistic simulation methods were examined by Pellenq et al. in order to ameliorate the mechanical properties of C-S-H [23]. Shahsavari et al., investigated the possibility of applying different force fields and effects of changing force fields them in the quality of simulation results. Based on a clay force field and calculations of bonds related to C-S-H paste and also computing the potential function by employing Density Functional Theory (DFT), and they introduced a new force field [24]. The aforementioned force field is also used by Qomi et. al. in order to optimize the properties of cement hydrates [25].

Tavakoli and Tarighat, investigated the mechanical properties of Portland cement phases [26]. Al-Ostaz et al., dealt with the mechanical properties of cement paste with two different force fields and could model and simulate the C-S-H, Calcium Hydroxide (CH), and other products of cement past [27]. Hajilar and Shafei investigated the usage of molecular dynamics in simulation of hydration products. So they could simulate the hydrated cement paste products and also made a comparison between their own findings and those existed in the pertinent literature [28].

In addition to the above-mentioned studies, employing atomistic simulation methods, other studies have recently been carried out concerning simulation of different properties of cement paste or concrete via various numerical methods [29-35].

In present study, firstly the modeling of famous Calcium silicate hydrate compounds was done and consequently, applying COMPASS, COMPASS II, ClayFF, INTERFACE and Universal force fields the molecular dynamics simulation were demonstrated. The Calcium silicate hydrate mechanical properties such as bulk modulus (K), shear modulus (G), Young's modulus (E) and Poisson's ratio (ν) were then computed for all the studied compounds and the obtained results were compared with those in the literature. In the next stage, the homogeneity process was carried out by applying Mori-Tanaka method and the amount of pores in C-S-H is noticed. This method makes it possible to examine the two types of C-S-H namely, LD and HD which in turn makes it possible to determine the more realistic nano structure of C-S-H. Finally, by introduced defects in structure, C-S-H structure was determined.

2. Materials and Method

2.1. C-S-H Compounds

Generally, it is believed that C-S-H is in charge of strength, durability and shrinkage of the Portland cement concrete [36]. The gel's structure is a layered structure which composed of silicate chains joined together in accordance with calcium oxide layers [37-40]. Due to the definition of unclear variable stoichiometry C-S-H forms are typically as the ratio of Ca/Si which is roughly about 1.2 to 2.1, for a hydrated Portland cement paste

[38], although C-S-H gel is an amorphous material, it has some short-range order at the atomic scale, and it has been revealed by comparing it with fully crystalline Calcium Silicate Hydrates [8].

Among more than 30 different known crystalline C-S-H [7], the tobermorite and jennite have many similarities to the C-S-H gel [41, 42]. Moreover, wollastonite group indicates some similarities with the C-S-H gel, however, it has different Ca/Si ratio rather than tobermorite and jennite [38].

Tobermorite as a calcium hydrate mineral has four structural varieties including: clinotobermorite, tobermorite 9 Å, tobermorite 11 Å, tobermorite 14 Å. The notations 9Å, 11Å, and 14Å show the characteristic basal spacing of 9.3, 11.3, and 14.0 Å, which is a function of the degrees of hydration [40].

By a dehydration process on progressive heating, tobermorite 14 Å, the most hydrated variety of the family, evolves to tobermorite 11 Å and later to tobermorite 9 Å [43].

The Ca/Si ratio of tobermorite 9 Å ($Ca_5Si_6O_{16}(OH)_2$) is 0.8 and its structure contains calcium layers which are similar to each other in comparison to the other kinds of tobermorites. The unit cell of tobermorite 9 Å is triclinic with C1 space group.

Tobermorite 11 Å, has a chemical constitution ranging from $Ca_5Si_6O_{17}.5H_2O$ to $Ca_4Si_6O_{15}$ $(OH)_2.5H_2O$ [40]. It has two distinct structures: Hamid structure which describes the tobermorite as independent layers [44] and Merlino structure which deliberates tobermorite as chemically bonded layers [41].

It is noteworthy to mention thatthe Merlino structure with $Ca_9O_{34}Si_{12}.10\ H_2O$ empirical formula is employed in the present study. It has a monoclinic unit cell with B11m space group. The Ca/Si ratio of tobermorite 11 Å in this study is 0.75.

Tobermorite 14 Å ($Ca_5Si_6O_{16}(OH)_2.7H_2O$) has a monoclinic unit cell with space group B11b and its Ca/Si ratio is 0.83 [45].

Clinotobermorite, $Ca_5Si_6O_{17}.5H_2O$, also has a monoclinic unit cell with Cc or C2/c_space group.

The crystal structures of tobermorite group are presented in fig. 1.

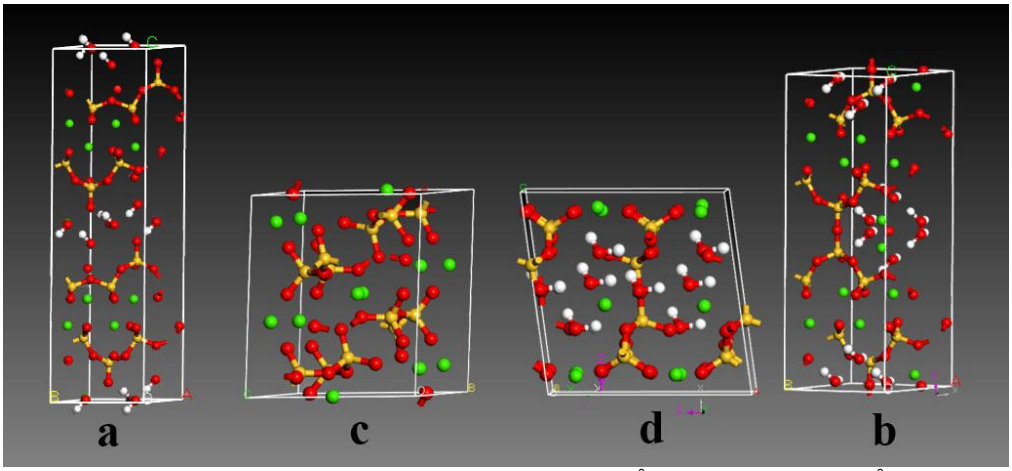

Fig. 1. Crystal structure of tobermorite group, a: tobermorite 14Å, b: tobermorite 11Å, c: tobermorite 9 Å, d: clinotobermorite – (white spheres: hydrogen ions; red spheres: Oxygen atoms; yellow spheres: silicon atoms; green spheres: calcium ions).

The chemical composition of jennite is $Ca_9Si_6O_{18}(OH)_6.8H_2O$ and it has dreierkette silicate chains like tobermorite [46]. The unit cell of jennite is triclinic with $P\bar{1}$ space group. Jennite has higher Ca/Si ratio (Ca/Si=1.5) rather than tobermorite and it is much closer to the ratio of hydrated cement in reality [47, 48]. The crystal structures of jennite is illustrated in fig. 2.

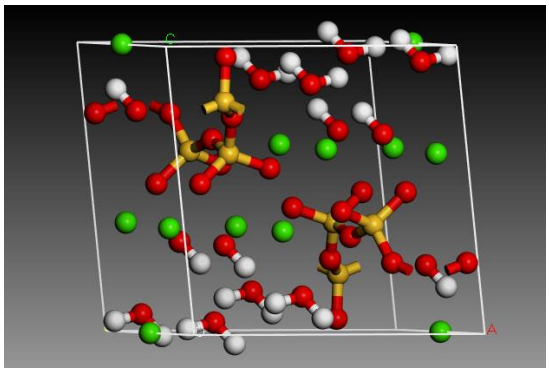

Fig. 2. Crystal structure of jennite – (white spheres: hydrogen ions; red spheres: Oxygen atoms; yellow spheres: silicon atoms; green spheres: calcium ions).

There are some other well-known C-S-H structures like foshagite, okenite, wollastonite, afwillite and jaffeite that studied in this study.

Foshagite composition is $Ca_4H_2O_{11}Si_3$ and it has triclinic unit cell with $P\bar{1}$ space group. The Ca/Si ratio of foshagite is 1.3 [49]. Okenite $Ca_{10}Si_{18}O_{46}.18H_2O$ is also a hydrated calcium silicate with the Ca/Si ratio of 0.55 and it is not a metamorphosed limestone [50]. Okenite_is triclinic_minerals with $P\bar{1}$ space group [51]. Wollastonite, $CaSiO_3$ crystallizes triclinically in space group $P\bar{1}$ is a calcium inosilicate mineral [52]. The structure of afwillite ($Ca_3(SiO_3OH)_2 \cdot 2H_2O$) is monoclinic with Cc space group. The Ca/Si ratio of afwillite is 1.5 [53]. Jaffeite $Ca_6Si_2O_7(OH)_6$ is also an hydrated calcium silicate. It has unit cell with P3 space group.

The Ca/Si ratio of jaffeite is 3 [54]. The crystal structures of these C-S-H compounds are presented in fig. 3.

It is noteworthy to mention that in this paper, different C-S-H crystals with the Ca/Si ranges from 0.5 to 3 and W/Si from 0 to 1.8 were analyzed.

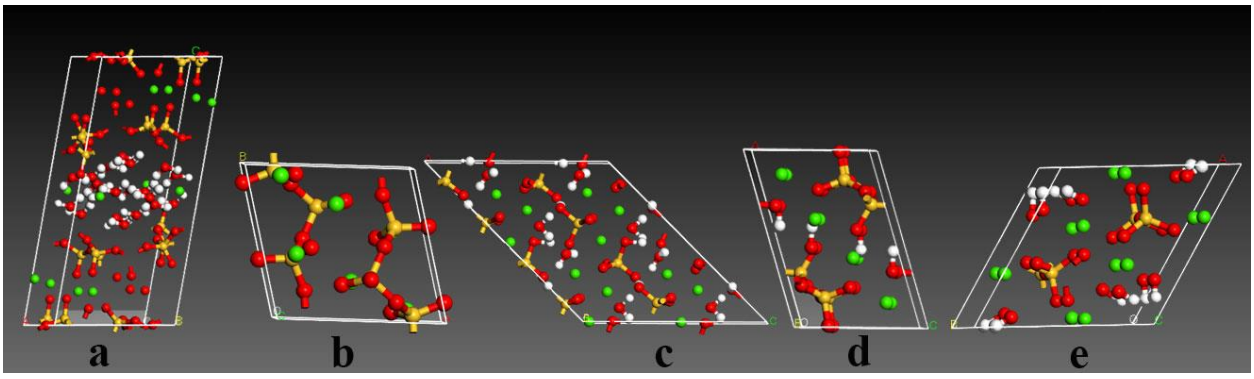

Fig. 3. Crystal structure of C-S-H compounds (a: okenite, b: wollastonite, C: afwillite, d: foshagite, e: jaffeite) **-** (white spheres: hydrogen ions; red spheres: Oxygen atoms; yellow spheres: silicon atoms; green spheres: calcium ions).

The Ca/Si and W/Ca of the above hydrated calcium silicates compound are highlighted in table 1.

Table 1. The Ca/Si and W/Ca ratio of C-S-H compounds.

	Okenite	tobermorite 11 Å	tobermorite 9 Å	tobermorite 14 Å	clinotobermorite
Ca/Si	0.55	0.75	O.8	0.8	0.83
W/Ca	1.8	1.11	0	1.4	1
	wollastonite	Foshagite	afwillite	jennite	jaffeite
Ca/Si	1	1.3	1.5	1.5	3
W/Ca	0	0	0.66	0.89	0

2.2. Simulation Methodology

In this paper, in order to explore the mechanical properties of C-S-H, the molecular dynamics method was performed [55]. It is consequential to select an appropriate force fields in molecular dynamics simulation.

In this paper COMPASS family (COMPASS and COMPASSII), Universal, ClayFF and INTERFACE Force fields were applied.

Pursuant to a review of the literature, the COMPASS (Condensed-phase Optimized Molecular Potentials for Atomistic Simulation Studies) force field has been employed to model different cementitious materials and had good results for mechanical properties [26-28, 56-59]. COMPASSII is an extension to the COMPASS force field. COMPASSII extends the existing coverage of COMPASS to include a significantly larger number of compounds of interest to researchers investigating ionic liquids [58, 60].

Universal is a purely diagonal, harmonic force field. Universal covers a full periodic Table. This is most significant advantage of this force filed. [57, 61].

ClayFF is an appropriate force field for simulations of hydrated crystalline compounds and their interfaces with liquid phases [24, 62- 64].

INTERFACE force filed has been developed recently for some compounds. In literatures the force field parameters for Tobermorite 11Å and Tobermorite 14Å have been introduced [65, 66].

Before starting the simulations, it is essential to minimize the structures and acquire energy optimized structures MD was performed when structure was minimized. Table 2 is shown simulation details in present study.

Table. 2. Simulation details.

Parameters	**Condition in this work**
Force fields	COMPASS, COMPASS II, Universal, ClayFF, INTERFACE
Ensemble	NPT
Summation method	Ewald
Cut-off distance	12.5Å
Temperature	298 K (Room temperature)
Temperature control (MD)	Nosé thermostat
Pressure	0.0001 GPa (Air pressure)
Pressure control	Berendsen barostat
Dynamic time (MD)	200 ps to 400 ps (based on the number of atoms)
Time step (MD)	1 fs
Boundary conditions	Three dimension periodic boundary condition (PBC)
Maximum strain amplitude in each strain configuration	0.003
Energy minimization process	Smart minimizer method (a steepest descent + conjugate gradient + Newton–Raphson methods)

The crystalline structure of all compounds is modeled and their lattice parameters have been summarized in Table 3. It is obvious that the differences of supercell features after molecular dynamics simulation in terms of experimental results are slight.

Table 3. Crystallographic lattice parameters of simulated C-S-H compounds.

		T9Å[a]	**T11Å[b]**	**14Å[c]**	**CT**	**Jen.**	**Fosh.**	**Oke.**	**Wol.**	**Afw.**	**Jaf.**
a (Å)	EXP	11.15	6.73	6.73	11.27	10.57	10.32	9.69	7.92	16.27	10.03
	COM.	10.36	6.44	6.36	10.31	9.42	9.07	9.43	7.16	14.98	8.56
	COMII	10.68	6.63	6.74	10.78	10.17	9.71	9.58	7.52	15.74	9.32
	ClayFF	11.03	6.74	6.72	11.12	10.35	10.21	9.86	7.82	16.09	10.13
	Uni.	11.67	7.20	6.97	11.62	11.22	10.81	10.03	8.26	18.21	10.86
	INTER	-	6.91	6.69	-	-	-	-	-	-	-
b (Å)	EXP	7.30	7.36	7.42	7.34	7.26	7.36	7.28	7.32	5.63	10.03
	COM.	6.78	7.05	7.01	6.72	6.47	6.47	7.08	6.61	5.18	8.56
	COMII	6.99	7.26	7.43	7.02	6.98	6.93	7.19	6.94	5.44	9.32
	ClayFF	7.22	7.38	7.41	7.24	7.11	7.28	7.41	7.22	5.56	10.13
	Uni.	7.64	7.88	7.68	7.57	7.71	7.70	7.54	7.63	6.30	10.86
	INTER	-	7.58	7.38	-	-	-	-	-	-	-
c (Å)	EXP	9.56	22.68	27.98	11.46	10.93	7.04	22.02	7.06	13.23	7.49
	COM.	8.88	21.70	26.42	10.49	9.73	6.19	21.43	6.38	12.18	6.40
	COMII	9.16	22.36	28.00	10.97	10.51	6.63	21.77	6.70	12.79	6.96
	ClayFF	9.46	22.73	27.95	11.31	10.69	6.96	22.41	6.97	13.08	7.57
	Uni.	10.01	24.27	28.98	11.82	11.60	7.37	22.80	7.36	14.81	8.11
	INTER	-	23.08	27.82	-	-	-	-	-	-	-
A (°)	EXP. & MD	101.08	90	90	99.18	101.3	90	92.7	90	90	90
B (°)	EXP. & MD	92.83	90	90	97.19	96.98	106.4	100.1	95.21	134.9	90
γ (°)	EXP. & MD	89.98	123.18	123.25	90	109.65	90	110.9	103.42	90	120

a[43] b[41] c[45] d[67] e[46] f[68] g[49] h[53] i[69] j[54]

Estimates of elastic properties of crystalline C-S-H models are computed by the energy minimization calculations [70]. The mechanical properties of materials were estimate with formulation which explained in ref. [26]. Voigt-Reuss-Hill (VRH) approximation was applied in order toappraise elastic properties [26, 40]. For estimate the elastic properties, Constant strain method was employed. The Constant strain method estimates the stiffness matrix by a series of finite difference approximations. This method starts by removing symmetry from the system, followed by an optional re-optimization of the structure, where the cell parameters can be varied. Optimization at this stage is always advised as incorrect results can be obtained if the structure is far from its lowest energy configuration. For each configuration, a number of strains are applied, resulting in a strained structure. The resulting structure is then optimized, keeping the cell parameters (and hence the strain) fixed, to allow for internal relaxation.

Simulations were carried out by the forcite module in Materials Studio software.

3. Results and Discussion

The elastic properties of all the C-S-H compounds have been acquired from MD simulations. Comparisons with the results of the other studies have been demonstrated in order to verify the accuracy of the simulations.

Dharmawardhana et al. [72] applied density functional theory (DFT) based ab initio analyses. Manzano [40] employed the molecular mechanics (MM) methods; Shahsavari et al. [24] performed the first-principles calculations using density functional theory (DFT); Hajilar & Shafei [28] utilized MD method, Oh et al. [19]

Employed experimental method, Pellenq et al. [23] used a classical potential energy minimization method, Al-Ostaz et al. [27] employed MD method, Janakiram Subramani [21] utilized molecular mechanics (MM) methods and Laugesen [73] applied DFT.

The mechanical properties for tobermorite group are presented in tables 4 to 7.

Table 4. Elastic properties of tobermorite 9Å.

Force field type	K (GPa)	G (GPa)	E (GPa)	ν
COMPASS FF	86.25	39.30	102.35	0.30
COMPASSII FF	82.00	26.75	72.38	0.35
Universal	53.36	36.23	88.63	0.23
Clay FF	135.93	68.83	176.67	0.28
Ref. value	78.09a, 68.95b, 71.42c, 70.88d	43.18a, 37.44b, 37.18c, 45.64d	109.39a, 95.11b, 95.06c, 112.72d	0.27a, 0.27b, 0.23d

a Dharmawardhana et al. [72]. b Manzano [40]. c Shahsavari et al. [24]. d Hajilar & Shafei [28].

Table 5. Elastic properties of tobermorite 11Å.

Force field type	K (GPa)	G (GPa)	E (GPa)	ν
COMPASS FF	71.56	26.76	71.40	0.33
COMPASSII FF	52.70	22.16	58.30	0.31
Universal	50.45	25.49	65.44	0.28
Clay FF	125.70	53.78	141.20	0.31
INTERFACE	38.45	17.91	46.5	0.29
Ref. value	77.19a, 73.57b, 66.65c, 64.40d	40.42[a], 29.19[b], 32.03[c], 35.24[d]	103.25[a], 77.34[b], 82.82[c], 89.40[d]	0.28[a], 0.32[b], 0.27[d]

a Dharmawardhana et al. [72]. b Manzano [40]. c Shahsavari et al. [24]. d Hajilar & Shafei [28].

Table 6. Elastic properties of tobermorite 14Å.

Force field type	K (GPa)	G (GPa)	E (GPa)	ν
COMPASS FF	43.93	18.81	49.38	0.31
COMPASSII FF	38.86	17.99	46.75	0.30
Universal	46.89	15.33	41.47	0.35
Clay FF	80.79	42.30	108.04	0.27
INTERFACE	46.53	28.89	71.80	0.24
Ref. value	56.42[a], 44.80[b], 47±4[c], 35.91[d], 20.7–35.4[e], 38.6[f], 55.74[g], 52.89[h]	31.65[a], 19.00[b], 19.0[c], 20.61[d], 2.78–5.08[e], 22.5[f], 26.67[g],18.55[h]	80.00[a], 49.94[b], 51.90[d], 63.5[e], 56.5[f], 69.01[g], 49.82h	0.26[a], 0.31[b], 0.25–0.26[e], 0.29[g], 0.34[h]

a Dharmawardhana et al. [72]. b Manzano [40]. c Oh et al. [19]. d Shahsavari et al. [24].
e Pellenq et al. [23]. f Richardson and Groves [38]. g Hajilar & Shafei [28]. h Al-Ostaz et al. [27].

Table 7. Elastic properties of clinotobermorite.

Force field type	K (GPa)	G (GPa)	E (GPa)	ν
COMPASS FF	71.59	30.96	81.17	0.31
COMPASSII FF	40.98	19.84	51.24	0.29
Universal	41.67	14.70	39.45	0.34
Clay FF	104.12	47.59	123.89	0.30
Ref. value	81.00[a]	35.00[a]	91.78[a]	0.31[a]

a Manzano [40]

For the tobermorite 9Å, ClayFF could not present acceptable results. The tobermorite 9Å Young's modulus applying COMPASS, COMPASSII and Universal was computed to be 102.35 GPa, 72.38 GPa and 88.63 GPa respectively. The results in the preceding works have been reported to be between 95 GPa and 113 GPa. Comparing the present study results with those of the related literature, it was concluded that the reported results by COMPASS are within the above-mentioned ranges. Universal and COMPASS II also have a good result. Furthermore, the acquired Young's modulus for tobermorite 11Å employing COMPASS, COMPASSII, Universal and INTERFACE were 71.4 GPa, 58.3 GPa, 65.44 GPa and 46.50 GPa respectively. Compared to previous studies, the results of Clay FF force fields were not appropriate. Results from COMPASS force field are close to the reported results [40]. However, it is noteworthy to mention that in the previous studies, tobermorite 11Å was applied with different Ca/Si ratios. Besides, the offered structure by Hamid and Merlino also differ from each other and in different studies each of them might be used. The calculated Young's modulus for tobermorite 11Å has been reported in the literature to be within 77 GPa and 104 GPa.

The reported Young's modulus for Tobermorite 14Å by COMPASS, COMPASSII and Universal was similar to each other (49.36 GPa, 46.75 GPa and 41.47). Deliberating the related literature, it is obvious that these findings are very close to previous literature [40], Shahsavari et al. [24], Al-Ostaz et al. [27], and Oh et al [19]. The reported Young's modulus in the previous studies for the same compound was between 49 GPa and 80 GPa. As it is clear, the results of the current study with COMPASS, COMPASS II and INTERFACE force fields are also in the same range and are in line with most of the previous studies. The acquired results by INTERFACE force field were also close to the findings of Pellenq et al. [23] and Hajilar & Shafei [28] respectively.

Young's modulus for clinotobermorite in the literature was reported just in one study [40]. Comparing these findings, it might be argued that the results by COMPASS force field are more similar to these results.

The MD results obtained for the crystalline structure of Jennite are presented in table 8.

Table 8. Elastic properties of jennite.

Force field type	K (GPa)	G (GPa)	E (GPa)	ν
COMPASS FF	61.56	21.74	58.35	0.34
COMPASSII FF	37.46	15.44	40.72	0.31
Universal	18.20	8.79	22.71	0.29
Clay FF	49.05	19.84	52.44	0.32
Ref. value	62.65[a], 40.20[b], 31.83[c], 32.0[d] 64.09[e], 69[f], 51[k]	35.02[a], 22.10[b], 21.96[c], 19.9[d], 31.31[e], 25f, 27[k]	88.56[a], 56.03[b], 53.55[c], 49.5[d], 80.77[e], 66.9[f], 69[k]	0.2752[a], 0.27[b] 0.29[e],0.34[f], 0.28[k]

a Dharmawardhana et al. [72]. b Manzano [40]. c Shahsavari et al. [24]. d Richardson and Groves [38]. e Hajilar & Shafei [28]. f Al-Ostaz et al. [27]. k Janakiram Subramani [21].

The reported Young's modulus for jennite in the previous studies was between 49.5 GPa and 88.5 GPa. However, in this study the same results were obtained, 58.35 GPa, 40.72 GPa and 52.44 GPa applying COMPASS, COMPASSII and Clay FF respectively. The obtained results by COMPASS and Clay FF force fields are similar to the existing results. They are the closer values to the works by Manzano [40] and Shahsavari et al. [24]. Besides, the obtained result by COMPASSII force field was close to the finding of Richardson and Groves [38] as well.

The Elastic properties for foshagite, okenite, wollastonite, afwillite and jaffeite, are summarized in Tables 9 –13, respectively.

Table 9. Elastic properties of foshagite.

Force field type	K (GPa)	G (GPa)	E (GPa)	ν
COMPASS FF	96.32	37.60	99.8	0.32
COMPASSII FF	69.00	27.63	73.12	0.32
Universal	43.05	23.07	58.72	0.27
Clay FF	36.06	27.24	65.28	0.2
Ref. value	73.70[a], 75[b]	40.0[a], 39[b]	101.62[a], 100[b], 110[c]	0.27[a], 0.28[b]

a Manzano [40]. b Janakiram Subramani [21]. c Laugesen [73].

Table 10. Elastic properties of okenite.

Force field type	K (GPa)	G (GPa)	E (GPa)	ν
COMPASS FF	43.44	21.49	55.34	0.28
COMPASSII FF	42.56	23.45	59.43	0.26
Universal	56.04	26.26	68.13	0.29
Clay FF	51.52	27.79	70.66	0.27
Ref. value	48.31a	22.85a	59.21a	0.30a

a Manzano [40].

Table 11. Elastic properties of wollastonite.

Force field type	K (GPa)	G (GPa)	E (GPa)	ν
COMPASS FF	105.89	36.08	97.20	0.34
COMPASSII FF	66.96	28.35	74.53	0.31
Universal	29.27	12.81	33.53	0.31
Clay FF	159.48	61.12	162.58	0.33
Ref. value	84.06[a]	41.59[a]	107.10[a]	0.29[a]

a Manzano [40].

Table 12. Elastic properties of afwillite.

Force field type	K (GPa)	G (GPa)	E (GPa)	N
COMPASS FF	73.21	22.27	60.66	0.36
COMPASSII FF	46.23	17.37	46.31	0.33
Universal	17.51	8.56	22.08	0.29
Clay FF	75.59	29.49	77.65	0.31
Ref. value	61.00[a]	25.00[a]	65.99[a]	0.32[a]

a Manzano [40].

Table 13. Elastic properties of jaffeite.

Force field type	K (GPa)	G (GPa)	E (GPa)	ν
COMPASS FF	131.48	37.93	103.80	0.36
COMPASSII FF	62.52	21.85	58.71	0.34
Universal	14.64	11.98	28.23	0.17
Clay FF	105.18	37.19	99.80	0.34
Ref. value	68.76[a]	39.08[a]	98.57[a]	0.26[a]

a Manzano [40].

The reported results for foshagite by formerly carried out studies employing MD and DFT methods was about 100. Comparing the previous results and the current study findings, it is clear that results by COMPASS force field is considerably similar to that of previous works. As with the okenite, the resulted Young's modulus by COMPASSII was equal to the only reported result [40]. Further, results from COMPASS and Universal were in the same range as well. The same reported result for wollastonite was 107.10 [40]. The acquired result in this study was 97.2 GPa by applying COMPASS. Likewise, the results of afwillite for Young's modulus were also found out to be 60.66 GPa and 77.65 GPa for the COMPASS and Clay FF force fields respectively. These Results were very close to the reported result [40]. The same results by COMPASS and Clay FF for jaffeite was also reported to be 103.80 GPa and 99.8 GPa that were very similar to the reported result [40].

The obtained results for K, G and ν indicate that the Findings of present study are close to those of previous studies and in the most cases the reported ranges by researchers employing different methods were in the same range with this study findings. Existing differences were mostly less than 10 percent. These slight differences are acceptable given the different simulation methods applied by different researchers and also using different

simulation hypotheses. However, the current study findings had the most similarity to the studies by Manzano (MM method) [40], Al Ostaz et al. (MD method) [27], and Shahsavari (DFT method) [24].

C-S-H is built of H_2O, SiO_2 and CaO. Actually, if each of the letters in C-S-H word be regarded as a component of the gel, Ca. Si and H are the major elements in C-S-H crystals. One good way to compare the C-S-H crystals is investigate the effect of percentage of elements on mechanical properties. Moreover, Ca/Si ratio has been consequentialparameter to characterize the properties of C-S-H. The Young's modulus as a function of Ca/Si, W/Ca, H%, Si%, O% and Ca% are illustrated in Fig. 4.

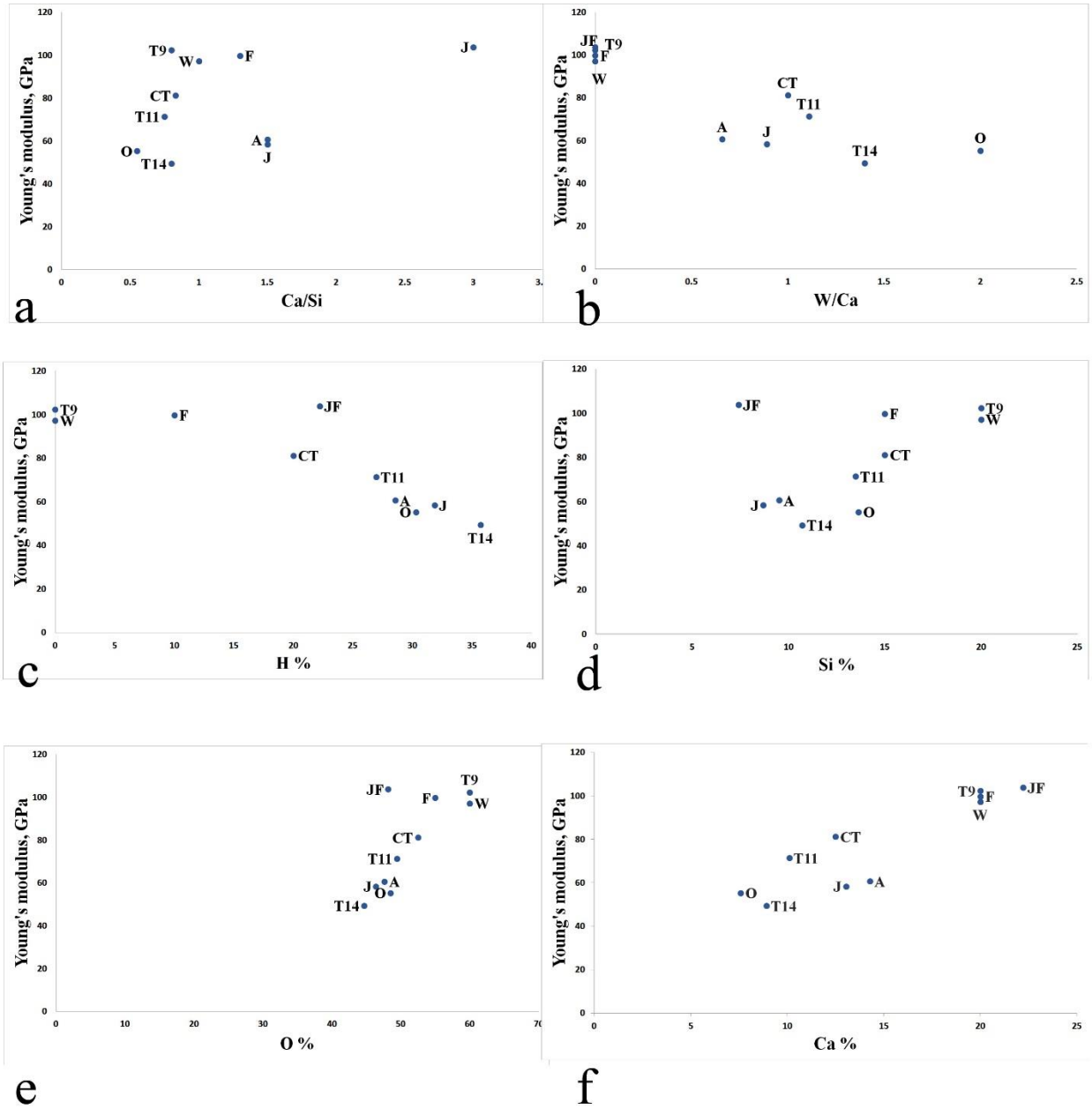

Fig.4. Young's modulus as a function of (a) Ca/Si, (b) W/Ca, (c) H% (d) Si% (e) O% and (f) Ca%.

Fig. 4 (a) indicates weak correlation for Ca/Si ratios. It has inconsistent trend. This contradictory trend also exhibited in deferent study: Contantinides et al. [74] and Plassard et al.[75] applying nano-indentation method for investigation of Ca/Si ratio. They resulted that the Young's modulus of calcium silicate hydrate increase with Ca/Si ratio. Alizadeh et al. [76] using dynamic mechanical analysis (DMA) for investigation of Ca/Si ratio. Contrary, they observed the exact opposite trend. Hence, more study on calcium silicate hydrate is needed to clear this issue. Figures 4 (b) and (c) for W/Ca ratio and H percentage reveal the downward trend. The Young's modulus reduction might be ascribed to the weakening of bonds as a result to the existence of water. Water increases the distance between calcium silicate layers. Water possesses space and in turn, increases the distance between layers. This results in reduction of columbic attraction between the neighboring silicate chains and related calcium. These actions lead to weakening of bonds and reducing of Young's modulus. Then again, water causes new hydrogen bonds to form and these new bonds cause more weakening among atoms. To put it simple, in C-S-H structure with more water, the strength and stable bonds between Ca and Oxygen in silicate chains are partially replaced by the unstable hydrogen bonds. Figures 4 (d), (e) and (f) indicate good correlation with rising trend for Si, O and Ca atomic percentage. The reason for this rising trend is probably increasing of powerful ionic bonds.

3.1. Microporomechanical Properties Calculation of LD and HD C–S–H

C–S–H gel is a porous material. The gel was pictured as a composite made of a solid phase with air void inclusions [13]. Pursuant to the literature reviews for the C-S-H gel (e.g., [16, 18]), in terms of gel porosity and packing density, the porosity of the HD and LD types of the C-S-H gel has been assumed equal to 0.25 and 0.35. Effective properties of heterogeneous materials can be evaluated roughly by several methods such as Mori-Tanaka Method and Self-Consistent approach. These methods are able to rescale the properties of the individual crystalline phases of the C–S–H to those of the C–S–H itself contemplating a number of parameters that represent the gel porosity and solid phases [77]. Among them, in this study, Mori-Tanaka (MT) homogenization method was applied to rescale the properties of crystalline phases to those of the C-S-H gel.

The MT method was essentially proposed to compute the elastic properties of a solid matrix with misfitting pore inclusions [78]. In consonance withthis method, the effective shear and bulk modulus of the C–S–H gel can be estimated applying the following equations [78]:

$$K_{\mathrm{CSH}} = K_{\mathrm{solid}} \frac{4G_{\mathrm{solid}}(1-\emptyset)}{3K_{\mathrm{solid}}\emptyset + 4G_{\mathrm{solid}}} \quad (1)$$

$$G_{\mathrm{CSH}} = G_{\mathrm{solid}} \frac{(1-\emptyset)(8G_{\mathrm{solid}} + 9K_{\mathrm{solid}})}{6\emptyset(2G_{\mathrm{solid}} + K_{\mathrm{solid}}) + 8G_{\mathrm{solid}} + 9K_{\mathrm{solid}}} \quad (2)$$

$\emptyset$ is the porosity of C-S-H gel, K and G are bulk modules and shear modules respectively. The calculated Young's modulus of C-S-H compounds are shown in Table 14. Young's modulus are computed only for the force fields that compare to literature had appropriate answer. The final results are compared with experimental methods [16,17,79] to verify the accuracy of the estimates which determined by microporomechanical equations. The young's

modulus reported by literature are about 30 GPa for HD and 20 GPa for LD C-S-H.

Comparing the results indicated in Table 14 with those of experimental studies in terms of Elastic properties of C-S-H, it can be found out that okenite, jennite and tobermorite 14Å have acceptable results within the range of previously acquired results. The wollastonite, jaffeite, foshagite, and tobermorite 9Å compounds have the largest difference from experimental results.

The resulted Young's modulus for tobermorite 14Å was in conformity with that of C-S-H reported in previous studies. This result is very close to the experimental results both for LD and HD cases and with both COMPASS and COMPASSII. Moreover, for tobermorite 14Å, COMPASS II force field led to better results in both of the LD and HD C-S-H. As it had also been reported in the previously carried out studies, it was expected that tobermorite 14Å has the most similarity to the C-S-H paste. The reported values in HD case with COMPASS II and in LD case with Universal were close to experimental results. However, these two force fields were acceptable with an error of below 10 %. Given this result and this degree of correspondence, it can be concluded that the obtained findings are valid and reliable.

Comparing the acquired results for jennite, it is proven that the Young's modulus is very close to the experimental results. It is also found that only in the case of applying Clay FF the results, in comparison with the experimental ones, have little errors and are acceptable. Similarly, the results for okenite had about 10 % error and were almost same as the acquired experimental results. Deliberating these results, tobermorite 14Å has the most similar structure to the C-S-H for mechanical properties.

Table 14. Young's modulus of the LD and HD C–S–H gels estimated based on Mori-Tanaka method**.**

Compound	Force field type	Young's modulus (GPa), LD	Young's modulus (GPa), HD
tobermorite 9 Å	COMPASS	49.22	61.35
	Universal	42.63	53.14
tobermorite 11 Å	COMPASS	34.37	42.83
tobermorite 14 Å	COMPASS	23.75	29.61
	COMPASS II	22.48	28.03
	Universal	19.98	24.90
	INTERFACE	35.52	43.04
Clinotobermorite	COMPASS	39.05	30.71
Jennite	COMPASS	28.10	35.02
	Clay FF	25.24	31.45
Foshagite	COMPASS	48.04	59.87
Okenite	COMPASS	26.61	33.17
Wollastonite	COMPASS	46.83	58.35
Afwillite	COMPASS	29.25	36.44
	Clay FF	31.75	39.57
Jaffeite	COMPASS	50.09	62.39
	Clay FF	48.07	59.90
experimental results of C-S-H gel		23.4±3.4a, 21.7±2.1b, 22.89c	31.4±2.1a, 29.4±2.4b, 31.16c

a Zhu et al. [17]. b Constantinides & Ulm [16]. C Mondal et al. [79].

4. Conclusion

The current study comprehensively dealt with the investigation of different compounds of C-S-H with a vast ratios of Ca/Si from 0.5 to 3. Ten types of C-S-H compounds including tobermorite 9Å, tobermorite 11Å, tobermorite 14Å, clinotobermorite, jennite, afwillite, okenite, jaffeite, foshagite, and wollastonite were selected and, after a primary modeling, were simulated by employing different force fields of COMPASS, COMPASSII, Clay FF, Universal and INTERFACE. It was done to calculate their mechanical properties such as G, K, E and ν. These properties were estimated by contemplating the results of MD simulations. After obtaining the early results, the porosity degree For C-S-H of LD and HD Kinds were computed by Mori-Tanaka method. Finally, with introducing defect in the structure, the C-S-H properties were determined.

The simulations results revealed that tobermorite 14Å is the most similar C-S-H material to the C-S-H gel in hydrated cement paste. Also, the simulation results of jennite shows the same similarity to the C-S-H gel as well. The acquired findings for elastic properties of these material were approximately same as the experimental results. Regarding the force fields, it was observed that the COMPASS family force field is satisfactory for MD simulations of C-S-H. The current study findings indicate that the molecular dynamics method can predict the mechanical properties of C-S-H with high accuracy. Moreover, it might be stated that this method, in comparison to the other methods, is more accurate and produce more similar results to experimental results.

Conflict of Interest

The authors declare that there is no conflict of interests regarding the publication of this manuscript.

REFRENCES

[1] Tavakoli, D., Hashempour, M., & Heidari, A. (2018). Use of Waste Materials in Concrete: A review. Pertanika Journal of Science & Technology, 26(2), 499-522.

[2] Tavakoli, D., Heidari, A., & Pilehrood, S. H. (2014). Properties of Concrete made with Waste Clay Brick as Sand Incorporating Nano SiO2. Indian Journal of Science and Technology, 7(12), 1899-1905.

[3] Taylor, H.F., Cement Chemistry. 2 ed. 1997, London: Thomas Telford Publishing.

[4] Tarighat, A., Zehtab, B., & Tavakoli, D. (2016). An introductory review of simulation methods for the structure of cementitious material hydrates at different length scales. Pertanika Journal of Science & Technology (JST), 24(1), 27-39.

[5] Papatzani, S., Paine, K., & Calabria-Holley, J. (2015). A comprehensive review of the models on the nanostructure of calcium silicate hydrates. Construction and Building Materials, 74, 219-234.

[6] Kar, A., Ray, I., Unnikrishnan, A., & Davalos, J. F. (2012). Estimation of C-S-H and calcium hydroxide for cement pastes containing slag and silica fume. Construction and Building Materials, 30, 505-515.

[7] Richardson, I. G. (2008). The calcium silicate hydrates. Cement and Concrete Research, 38(2), 137-158.

[8] Manzano, H., Dolado.J.S, Guerrero.A., & Ayuela.A. (2007) Mechanical properties of crystalline Calcium-silicate-hydrates: comparison with cementitious C-S-H gels, Phys. stat. sol. 204, 1775–1780.

[9] Selvam, R.P., Murray, S.J., Jankiram Subramani, V., & Hall, K.D. (2009) Potential application of nanotechnology on cement based materials, Report: Mack

Blackwell Transportation Center, University of Arkansas, MBTC DOT 2095/3004.

[10] Bankura, A., & Chandra, A. (2005). Hydration and translocation of an excess proton in water clusters: Anab initio molecular dynamics study. Pramana, 65(4), 763-768.

[11] Zehtab, B., & Tarighat, A. (2016). Diffusion study for chloride ions and water molecules in CSH gel in nano-scale using molecular dynamics: Case study of tobermorite. ADVANCES IN CONCRETE CONSTRUCTION, 4(4), 305-317.

[12] Zehtab, B., & Tarighat, A. (2017). Molecular dynamics simulation to assess the effect of temperature on diffusion coefficients of different ions and water molecules in CSH. Mechanics of Time-Dependent Materials, 1-15.

[13] Tavakoli, D., Tarighat, A., & Beheshtian, J. (2017). Nanoscale investigation of the influence of water on the elastic properties of C–S–H gel by molecular simulation. Proceedings of the Institution of Mechanical Engineers, Part L: Journal of Materials: Design and Applications, 1464420717740926.

[14] Tarighat, A., & Tavakoli, D. (2016). Estimation of mechanical properties of hardened cement paste with molecular dynamics simulation method at nano scale. Modares Mechanical Engineering, 16(6), 71-78.

[15] Hughes, J. J., & Trtik, P. (2004). Micro-mechanical properties of cement paste measured by depth-sensing nanoindentation: a preliminary correlation of physical properties with phase type. Materials characterization, 53(2), 223-231.

[16] Constantinides, G., & Ulm, F. J. (2007). The nanogranular nature of C–S–H. Journal of the Mechanics and Physics of Solids, 55(1), 64-90.

[17] Zhu, W., Hughes, J. J., Bicanic, N., & Pearce, C. J. (2007). Nanoindentation mapping of mechanical properties of cement paste and natural rocks. Materials characterization, 58(11), 1189-1198.

[18] Vandamme, M., Ulm, F. J., & Fonollosa, P. (2010). Nanogranular packing of C–S–H at substochiometric conditions. Cement and Concrete Research, 40(1), 14-26.

[19] Oh, J. E., Clark, S. M., Wenk, H. R., & Monteiro, P. J. (2012). Experimental determination of bulk modulus of 14Å tobermorite using high pressure synchrotron X-ray diffraction. Cement and Concrete Research, 42(2), 397-403.

[20] Faucon, P., Delaye, J.M., & Virlet, J. (1996) Molecular Dynamics Simulation of the Structure of Calcium Hydrates. Journal of Solid State Chemistry 127, 92–97.

[21] Janakiram Subramani, V., Murray, S., Panneer Selvam, R., & Hall, K. D. (2009). Atomic Structure of Calcium Silicate Hydrates Using Molecular Mechanics. In Transportation Research Board 88th Annual Meeting (No. 09-0200).

[22] Murray, S.J., Jankiram Subramani, V., Selvam, R.P., & Hall, K.D. (2010) Molecular dynamics to understand the mechanical behavior of cement paste. Transportation Research Record 2142, 75–82.

[23] Pellenq, R. M., Lequeux, N., & Van Damme, H. (2008). Engineering the bonding scheme in C–S–H: The iono-covalent framework. Cement and Concrete Research, 38(2), 159-174.

[24] Shahsavari, R., Pellenq, R.J.M., & Ulm, F.J. (2011) Empirical force fields s for complex hydrated calcio-silicate layered materials, Physical Chemistry Chemical Physics 13, 1002-1011.

[25] Qomi, M.J.A., Krakowiak, K.J., Bauchy, M., Stewart, K.L., Shahsavari, R., Jagannathan, D., Brommer, D.B., Baronnet, A., Buehler, M.J., Yip, S., Ulm, F.-J., Van Vliet, K.J., & Pellenq, R.J-.M. (2014) combinatorial molecular optimization of cement hydrates, Nature Comunications, 5:4960, DOI: 10.1038/ncomms5960

[26] Tavakoli, D., & Tarighat, A. (2016). Molecular dynamics study on the mechanical properties of Portland cement

clinker phases. Computational Materials Science, 119, 65-73.

[27] Al-Ostaz, A., W. Wu, AH-D. Cheng, and C. R. Song. "A molecular dynamics and microporomechanics study on the mechanical properties of major constituents of hydrated cement." Composites Part B: Engineering 41, no. 7 (2010): 543-549.

[28] Hajilar, S., & Shafei, B. (2015) Nano-scale investigation of elastic properties of hydrated cement paste constituents using molecular dynamics simulations. Computational Materials Science 101, 216-226.

[29] Bullard J.W., Virtual Cement and Concrete Testing Laboratory (VCCTL) user guide.: Materials and Construction Research Division National Institute of Standards and Technology Gaithersburg, Maryland USA (2011).

[30] van Breugel K., Numerical simulation of hydration and microstructural development in hardening cement-based materials (I) Theory.: Cement and Concrete Research, 25(2) (1995) 319-331.

[31] Koenders E.A.B. and van Breugel K., Numerical modeling of autogenous shrinkage of hardening cement paste.: Cement and Concrete Research, 27(10) (1997) 1489-1499.

[32] Bishnoi Sh., Vector Modelling of Hydrating Cement Microstructure and Kinetics.: PhD thesis, EPFL university, Switzerland, (2009).

[33] Maekawa K., Chaube R.P., and Kishi T., Modelling of Concrete Performance.: London, E&FN SPON. (1999).

[34] Koenders E.A.B., Schlangen E., and van Breugel K., Multi-scale modeling: The Delft Code.: International RILEM symposium on concrete modeling-CONMOD'08, 26-28 May 2008, Delft, The Netherlands.

[35] Zhang M., Multiscale Lattice Boltzmann-Finite Element Modelling of Transport Properties in Cement-based Materials.: PhD thesis, Delft university, the Netherlands, (2013).

[36] Hou, D. (2014). Molecular simulation on the calcium silicate hydrate (CSH) gel.

[37] Plassard, C., Lesniewska, E., Pochard, I., & Nonat, A. (2004). Investigation of the surface structure and elastic properties of calcium silicate hydrates at the nanoscale. Ultramicroscopy, 100(3), 331-338.

[38] Richardson, I.G. and G.W. Groves, Models for the composition and structure of calcium silicate hydrate (C-S-H) gel in hardened tricalcium silicate pastes. Cement and Concrete Research, 1992. 22(6): p. 1001-1010.

[39] Richardson, I.G., The nature of the hydration products in hardened cement pastes. Cement & Concrete Composites, 2000. 22(2): p. 97-113.

[40] Manzano Moro, H. (2014). Atomistic simulation studies of the cement paste components. Servicio Editorial de la Universidad del País Vasco/Euskal Herriko Unibertsitatearen Argitalpen Zerbitzua.

[41] Merlino, S., Bonaccorsi, E., & Armbruster, T. (2001). The real structure of tobermorite 11Å normal and anomalous forms, OD character and polytypic modifications. European Journal of Mineralogy, 13(3), 577-590.

[42] Richardson, I. G. (2004). Tobermorite/jennite-and tobermorite/calcium hydroxide-based models for the structure of CSH: applicability to hardened pastes of tricalcium silicate, β-dicalcium silicate, Portland cement, and blends of Portland cement with blast-furnace slag, metakaolin, or silica fume. Cement and Concrete Research, 34(9), 1733-1777.

[43] Merlino, S., Bonaccorsi, E., & Armbruster, T. (1999). Tobermorites: Their real structure and order-disorder (OD) character. American Mineralogist, 84, 1613-1621.

[44] Hamid, S.A., The crystal structure of 11Å natural tobermorite Ca2.25[Si3O7.5(OH)1.5]• 1 H2O. Zeitschrift Fur Kristallographie, 1891. 154: p. 189-198.

[45] Bonaccorsi, E., S. Merlino, and A.R. Kampf, The crystal structure of tobermorite 14Å (Plombierite), a C-S-H phase. Journal of the American Ceramic Society, 2005. 88(3): p. 505-512.

[46] Bonaccorsi, E., Merlino, S., & Taylor, H. F. W. (2004). The crystal structure of jennite, Ca9 Si6O18(OH)6•8H2O. Cement and Concrete Research, 34(9), 1481-1488.

[47] Carpenter, A.B.; Chalmers, R.A.; Gard, J.A.; Speakman, K.; Taylor, H.F.W. (1966), "Jennite, a new mineral" , American Mineralogist 51: 56–74, retrieved 2009-02-04.

[48] Li, Z. (2011). Advanced concrete technology. John Wiley & Sons.

[49] Gard, J. A., & Taylor, H. F. W. (1960). The crystal structure of foshagite. Acta Crystallographica, 13(10), 785-793.

[50] Gard, J. A., & Taylor, H. F. W. (1956). Okenite and nekoite (a new mineral). Mineral. Mag, 31, 5-20.

[51] Merlino, S. (1983). Okenite, Ca10Si18O46.18H2O; the first example of a chain and sheet silicate. American Mineralogist, 68(5-6), 614-622.

[52] Ohashi, Y. and L.W. Finger, Role of octahedral cations in pyroxenoid crystal chemistry. 1. Bustamite, wollastonite and pectolite-schizolite-serandite series. American Mineralogist, 1978. 63(3-4): p. 274-288.

[53] Malik, K. M. A., & Jeffery, J. W. (1976). A re-investigation of the structure of afwillite. Acta Crystallographica Section B: Structural Crystallography and Crystal Chemistry, 32(2), 475-480.

[54] Yamnova, N. A., Sarp, K., Egorov-Tismenko, Y. K., Pushcharovski, D., & Dasgupta, G. (1993). Crystal structure of jaffeite. Crystallography reports, 38(4), 464-467.

[55] Alder, B. J.; T. E. Wainwright (1959). "Studies in Molecular Dynamics. I. General Method". J. Chem. Phys. 31 (2): 459.

[56] Shu, Xin, et al. "Tailoring the solution conformation of polycarboxylate superplasticizer toward the improvement of dispersing performance in cement paste." Construction and Building Materials 116 (2016): 289-298.

[57] Wu, W., Al-Ostaz, A., Cheng, A. H. D., & Song, C. R. (2011). Computation of elastic properties of Portland cement using molecular dynamics. Journal of Nanomechanics and Micromechanics, 1(2), 84-90.

[58] Accelrys Inc. Materials studio 7.0 software. San Diego (CA); 2007

[59] COMPASS: an ab initio force-field optimized for condensed-phase applications overview with details on alkane and benzene compounds. The Journal of Physical Chemistry B, 102(38), 7338-7364.

[60] Mayo, S. L., Olafson, B. D., & Goddard, W. A. (1990). DREIDING: a generic force field for molecular simulations. Journal of Physical Chemistry, 94(26), 8897-8909.

[61] Rappé, A. K., Casewit, C. J., Colwell, K. S., Goddard Iii, W. A., & Skiff, W. M. (1992). UFF, a full periodic table force field for molecular mechanics and molecular dynamics simulations. Journal of the American Chemical Society, 114(25), 10024-10035.

[62] Cygan, R.T., J.J. Liang, and A.G. Kalinichev, Molecular models of hydroxide, oxyhydroxide, and clay phases and the development of a general force field. Journal of Physical Chemistry B, 2004. 108(4): p. 1255-1266.

[63] Galmarini, S. C. (2013). Atomistic simulation of cementitious systems.

[64] Dauber-Osguthorpe, P., Roberts, V. A., Osguthorpe, D. J., Wolff, J., Genest, M., & Hagler, A. T. (1988). Structure and energetics of ligand binding to proteins: Escherichia coli dihydrofolate reductase-trimethoprim, a drug-receptor system. Proteins: Structure, Function, and Bioinformatics, 4(1), 31-47.

[65] Mishra, R. K.; Flatt, R. J.; Heinz, H. Force Field for Tricalcium Silicate and Insight into Nanoscale Properties: Cleavage, Initial Hydration, and Adsorption of

Organic Molecules. J. Phys. Chem. C 2013, 117, 10417-10432.

[66] Mishra, R. K.; Fernandez-Carrasco, L.; Flatt, R. J.; Heinz, H. A Force Field for Tricalcium Aluminate to Characterize Surface Properties, Initial Hydration, and Organically Modified Interfaces in Atomic Resolution. Dalt. Trans. 2014, 43, 10602-10616.

[67] Merlino, S., Bonaccorsi, E., & Armbruster, T. (2000). The real structures of clinotobermorite and tobermorite 9 Å OD character, polytypes, and structural relationships. European Journal of Mineralogy, 12(2), 411-429.

[68] Merlino, S., Okenite, Ca10Si18O46 •18H2O - The first example of a chain and sheet silicate. American Mineralogist, 1983. 68(5-6): p. 614-622.

[69] Ohashi, Y., Polysynthetically-twinned structures of enstantite and wollastonite. Physics and Chemistry of Minerals, 1984. 10(5): p. 217-229.

[70] Haecker, C., et al., Modeling the linear elastic properties of Portland cement paste. Cement and Concrete Research, 2005. 35(10): p. 1948-1960.

[71] Hill, R. (1952). The elastic behaviour of a crystalline aggregate. Proceedings of the Physical Society. Section A, 65(5), 349.

[72] Dharmawardhana, C. C., Misra, A., Aryal, S., Rulis, P., & Ching, W. Y. (2013). Role of interatomic bonding in the mechanical anisotropy and interlayer cohesion of CSH crystals. Cement and Concrete Research, 52, 123-130.

[73] Laugesen, J. L. (2004). Density functional calculation of elastic properties of portlandite and foshagite. SPECIAL PUBLICATION-ROYAL SOCIETY OF CHEMISTRY, 292, 185-192.

[74] Constantinides, G., & Ulm, F. J. (2004). The effect of two types of CSH on the elasticity of cement-based materials: Results from nanoindentation and micromechanical modeling. Cement and concrete research, 34(1), 67-80.

[75] C. Plassard, E. Lesniewska, I. Pochard, and A. Nonat, “Intrinsic Elastic Properties of Calcium Silicate Hydrates by Nanoindentation”; in Proceedings of the 12th International Congress on the Chemistry of Cement, 2007

[76] R. Alizadeh, J. J. Beaudoin, and L. Raki, “Viscoelastic Nature of Calcium Silicate Hydrate,” Cement Concr. Compos., 32 [5] 369–76 (2010).

[77] Dormieux, L., D. Kondo, and F.J. Ulm, Microporomechanics. 2006: John Wiley & Sons.

[78] Mori, T., & Tanaka, K. (1973). Average stress in matrix and average elastic energy of materials with misfitting inclusions. Acta metallurgica, 21(5), 571-574.

[79] Mondal, P., Shah, S. P., & Marks, L. (2007). A reliable technique to determine the local mechanical properties at the nanoscale for cementitious materials. Cement and Concrete Research, 37(10), 1440-1444.